Influence of the Calcium-Induced Gel Phase on the Behavior of Small Molecules in Phosphatidylserine and Phosphatidylserine–Phosphatidylcholine Multilamellar Vesicles†

Kathryn I. Florine and Gerald W. Feigenson*
Section of Biochemistry, Molecular and Cell Biology, Cornell University, Ithaca, New York 14853
Received September 3, 1986; Revised Manuscript Received November 20, 1986

ABSTRACT: The behavior of fluorescent and spin-label probes is examined in several fluid and gel phospholipid phases, with particular focus on the Ca^{2+}-induced gel phase in phosphatidylserine (PS). These probes have behavior characteristic of the type of probe and of the type of lipid environment. Anthroyloxy- and doxyl-labeled PS [12-AS-PS and (7,6)PS, respectively] exhibit greatly restricted and/or slow probe motion in $Ca(PS)_2$, even compared to thermotropic gel-phase lipid at the same temperature. In contrast, anthroyloxy- and doxyl-labeled phosphatidylcholine (PC), as well as fluorescent-labeled and spin-labeled fatty acid derivatives, show no apparent change in probe motion in $Ca(PS)_2$ compared to fluid lamellar lipid. Doxyl-labeled phosphatidic acid, phosphatidylethanolamine, and phosphatidylglycerol show restricted motion in $Ca(PS)_2$ relative to fluid-phase lipid, but the electron paramagnetic resonance (EPR) spectra could not be interpreted in terms of simple models for probe ordering. The fluorescent probes diphenylhexatriene (DPH) and *trans*-parinaric acid methyl ester (tPNA-Me) show motional behavior in $Ca(PS)_2$ that is intermediate between that observed in fluid and in thermotropic gel-phase lipid. When $Ca(PS)_2$ and fluid PS/PC phases coexist, probe molecules distribute between the two phases. Experiments using fluorescence quenching by spin-labeled PC in PS/PC in excess Ca^{2+} yield the distribution of several fluorophore probes between fluid liquid-crystal and $Ca(PS)_2$ gel phases, expressed as a concentration ratio, $R_{LC/G}$. The value of $R_{LC/G} = 100$ in favor of the fluid phase is obtained for 12-AS-PC, 18 for 12-AS-Me, 12 for DPH, 3 for tPnA-Me, and 1 for 12-AS-PS. EPR spectral simulations yield $R_{LC/G} = 0.45$ for (7,6)PS in PS/PC in excess Ca^{2+}.

The interactions of Ca^{2+} with negatively charged phospholipids in biological membranes may play an important role in membrane fusion phenomena. One possibility for such a role, proposed by Papahadjopoulos et al. (1977), involves the interaction of Ca^{2+} with membrane lipids to induce a close apposition of two separate bilayer membranes and the lateral phase separation of acidic phospholipids within a membrane into rigid domains.

Phosphatidylserine (PS),[1] which can be present in significant amounts in real biological membranes, is often used in simple model membranes, alone or in combination with other lipids. PS binds Ca^{2+}, resulting in lipid phase changes and lipid vesicle aggregation and fusion (Portis et al., 1979; Ohnishi & Tokutomi, 1981; Uster & Deamer, 1981; Wilschut et al., 1981; Hoekstra, 1982; Ohki, 1982, 1984; Bentz et al., 1982; Hui et al., 1983; Morris et al., 1983; Düzgünes et al., 1984; Silvius & Gagné, 1984a,b; Tilcock et al., 1984; Rand et al., 1985; Parente & Lentz, 1986). Ca^{2+} binding between PS lamellae has been shown to produce a phase of low water content and highly ordered acyl chains (Portis et al., 1979). The composition of this phase is $Ca(PS)_2$ (Feigenson, 1986).

The $Ca(PS)_2$ phase appears to be different from a thermotropic gel phase. Differential scanning calorimetry reveals a "melting" temperature, in excess of 100 °C, that is essentially independent of acyl chain length (Hauser & Shipley, 1984). X-ray diffraction patterns show a very short lamellar repeat spacing, suggesting a nearly anhydrous state, as well as sharp lines in the wide-angle region indicative of acyl chain crystallization, which are not found for the hydrated PS thermotropic gel phase (Portis et al., 1979; Hauser & Shipley, 1984). However, there have been no previous reports of the behavior of probe molecules in the $Ca(PS)_2$ phase.

We have used a model system of multilamellar vesicles composed of PS or PS/PC and have examined the effects of Ca^{2+} binding between lamellae, on fluorescent and spin-label probes incorporated in the vesicles. Since Ca^{2+} binding between lamellae, bridging head groups, is different from surface binding at the aqueous interface [compare McLaughlin et al. (1981) with Feigenson (1986)], we believe that the vesicle–vesicle contact region of fusing biological membranes is best

† This work was supported by grants from the National Institutes of Health, U.S. Public Health Service (HL18255), and the National Science Foundation (DMB-85-10189) to G.W.F.

[1] Abbreviations: PS, 1,2-diacyl-*sn*-glycero-3-phosphoserine; PC, 1,2-diacyl-*sn*-glycero-3-phosphocholine; DOPS, 1,2-dioleoyl-*sn*-glycero-3-phosphoserine; DMPS, 1,2-dimyristoyl-*sn*-glycero-3-phosphoserine; BBPS, 1,2-diacyl-*sn*-glycero-3-phosphoserine derived from bovine brain; DOPC, DLPC, DMPC, DPPC, and DSPC, 1,2-dioleoyl-, 1,2-dilauroyl-, 1,2-dimyristoyl-, 1,2-dipalmitoyl-, and 1,2-distearoyl-*sn*-glycero-3-phosphocholine, respectively; PDPC, 1-palmitoyl-2-docosahexaenoyl-*sn*-glycero-3-phosphocholine; (7,6)-palmitic acid, 2-(6-carboxyhexyl)-2-octyl-4,4-dimethyloxazolidinyl-3-oxy; (7,6)PC, (7,6)PS, (7,6)PA, (7,6)-PE, and (7,6)PG, 1-acyl-2-[(7,6)-palmitoyl]-*sn*-glycero-3-phosphocholine, -phosphoserine, -phosphoric acid, -phosphoethanolamine, and -phosphoglycerol, respectively; 12-DS-Me, 12-(4′,4′-dimethyloxazolidinyl-*N*-oxy)stearic acid methyl ester; TEMPO, 2,2,6,6-tetramethylpiperidine-1-oxyl; TEMPO palmitate, 2,2,6,6-tetramethyl-1-oxypiperidin-4-yl hexadecanoate; 12-AS-Me, 12-(9-anthroyloxy)stearic acid methyl ester; 12-AS-PS, 1-acyl-2-[12-(9-anthroyloxy)stearoyl]-*sn*-glycero-3-phosphoserine; 12-AS-PC, 1-acyl-2-[12-(9-anthroyloxy)stearoyl]-*sn*-glycero-3-phosphocholine; DPH, 1,6-diphenyl-1,3,5-hexatriene; tPnA-Me, 9,11,13,15-*all-trans*-octadecatetraenoic acid methyl ester; Hepes, *N*-(2-hydroxyethyl)piperazine-*N*′-2-ethanesulfonic acid; EPR, electron paramagnetic resonance; T_t, gel to fluid liquid-crystal phase transition temperature; S, order parameter; p, fluorescence polarization; r, fluorescence anisotropy; K_p, partition coefficient; $R_{LC/G}$, ratio of fluorophore concentration in the fluid liquid-crystal phase to that in the gel phase.

0006-2960/87/0426-1757$01.50/0

modeled by multilamellar rather than single-walled vesicles. With multilayers, essentially the entire sample, rather than a small part of it, comprises the region of interest.

Spectroscopic probe molecules provide information characteristic of the type of probe and the type of environment. Because of our interest in both the characteristics of the $Ca(PS)_2$ phase and also the behavior of membrane-bound molecules in the presence of the $Ca(PS)_2$ phase, we have used a range of probe molecules, including the well-studied fluorescent probes diphenylhexatriene (DPH), *trans*-parinaric acid methyl ester (tPnA-Me), and 12-(9-anthroyloxy)stearic acid methyl ester (12-AS-Me) and spin probes 12-doxylstearic acid methyl ester (12-DS-Me) and TEMPO palmitate. (Ester derivatives, rather than free fatty acids, were used in order to avoid direct interaction with Ca^{2+} at the high concentrations used in these experiments.) We have also synthesized and studied the fluorescent phospholipid probes 12-AS-PC and 12-AS-PS and the spin-labeled phospholipids (7,6)PC, (7,6)PS, (7,6)PA, (7,6)PG, and (7,6)PE.

An important characteristic of probe molecule behavior is the probe distribution between coexisting lipid phases. There are several reports that describe the distribution of fluorescent probes between gel and fluid lipid in terms of a partition coefficient (Lentz et al., 1976; Sklar et al., 1979; Yguerabide & Foster, 1979; London & Feigenson, 1981b; Welti & Silbert, 1982; Feigenson, 1983; Rintoul et al., 1986). We describe EPR experiments that characterize the lipid phase behavior of PS/PC multilayers in the presence of Ca^{2+}, as well as the partition behavior of a spin-label probe between coexisting $Ca(PS)_2$ and fluid lipid phases. Using a fluorescence quenching technique developed in this laboratory (London & Feigenson, 1981a,b), we also determine the distribution of five fluorescent probes between coexisting $Ca(PS)_2$ and fluid lipid phases.

Experimental Procedures

Materials. Bovine brain PS (BBPS), dioleoyl-PS (DOPS), dimyristoyl-PS (DMPS), dioleoyl-PC (DOPC), dimyristoyl-PC (DMPC), dipalmitoyl-PC (DPPC), and distearoyl-PC (DSPC) were purchased from Avanti Polar Lipids Inc. (Birmingham, AL). TEMPO palmitate, 12-DS-Me, tPnA-Me, and 12-AS-Me were obtained from Molecular Probes Inc. (Eugene, OR). DPH and TEMPO were from Aldrich Chemical Co. (Milwaukee, WI). Hepes buffer was from Sigma Chemical Co. (St. Louis, MO). Water was purified on a Milli-Q system (Millipore Laboratory Products, Bedford, MA). Organic solvents were of HPLC grade. All other chemicals were of reagent grade.

Spin-labeled phospholipids were synthesized with a doxyl free radical on the eighth carbon of the 2-position fatty acyl group. (7,6)PC was prepared by condensation of (7,6)-palmitic acid with egg lyso-PC as described previously (London & Feigenson, 1981a). Other spin-labeled phospholipids were synthesized from (7,6)PC by phospholipase D catalyzed head group exchange, according to the method of Comfurius and Zwaal (1977). The fluorescent phospholipids 12-AS-PC and 12-AS-PS were prepared from 12-(9-anthroyloxy)stearic acid in an analogous manner.

Lipid purity was established by thin-layer chromatography on Adsorbosil Plus P plates (Applied Science, State College, PA). The solvent systems were chloroform/methanol/water (65:25:4 v/v) and chloroform/methanol/concentrated ammonium hydroxide (66:30:6 v/v). In addition, chloroform/acetone/methanol/acetic acid/water (6:8:2:2:1 v/v) was used to resolve (7,6)PE and (7,6)PG. The fluorescent probes tPnA-Me and 12-AS-Me were checked for free fatty acid contamination with hexane/ether/acetic acid [17:4:2 and 90:10:1 (v/v), respectively]. Loading was 10–20 μg for fluorophores and spin-labels and 50–100 μg for unlabeled lipids. All lipids and probes were judged to be >98% pure.

Choice of Phospholipids. Initial experiments utilized vesicles composed of BBPS and (7,6)PC, in which freezing in liquid N_2 was used to equilibrate Ca^{2+} between lamellae. To determine whether the freeze–thaw process itself affects the probes and/or lipids, EPR and fluorescence quenching experiments were performed on PS/PC samples that were subjected to either zero or else three freeze–thaw cycles. The samples that had been frozen in liquid N_2 exhibited irreversible bulk phase separation, as judged by changes in the EPR spectra for all mole fractions of (7,6)PC investigated (0.10–0.50) and significantly decreased quenching of DPH fluorescence by (7,6)PC over the same range of (7,6)PC concentration. Since freezing in liquid N_2 lowers the temperature well below the gel to liquid-crystal phase transition temperature (T_t) of the component lipids [T_t = −1 to 15 °C for BBPS (Boggs et al., 1977)], a new Ca^{2+} equilibration procedure was adopted, with freezing at −10 °C and use of only lipids with T_t <−10 °C. The lipids chosen were DOPS, T_t = −11 °C (Browning & Seelig, 1980; Martin Caffrey, unpublished experiments), DOPC, T_t = −22 °C (Ladbrooke & Chapman, 1969), and (7,6)PC, T_t = −30 to −40 °C (Martin Caffrey, unpublished experiments). With the above protocol, no bulk phase separation due to freezing was observed, as judged by superimposable fluorescence quenching curves for all probes in DOPS/(7,6)PC ± 15 freeze–thaw cycles and superimposable EPR spectra of DOPS/(7,6)PC ± 15 freeze–thaw cycles for all mole fractions of (7,6)PC.

Sample Preparation. Samples for fluorescence experiments were prepared under dim light as follows. Aliquots of stock solutions of DPH, 12-AS-Me, 12-AS-PC, or 12-AS-PS in chloroform or tPnA-Me in hexane were added to phospholipid in chloroform in 13 × 100 mm borosilicate culture tubes. Samples were then dried to a thin film under a stream of argon gas with gentle heating (35–40 °C), except for those containing tPnA-Me, which were dried at room temperature. Residual solvent was removed by vacuum pumping overnight in the dark. Buffer (10 mM Hepes, 100 mM KCl, pH 7.0) was added to give a total lipid concentration of 2 mM for DPPC samples or 4 mM for DOPS/(7,6)PC samples. Tubes were flushed with argon, sealed, and incubated for 30–60 min at 43 °C (DPPC samples) or room temperature (all others) in the dark, followed by several brief pulses of vortex mixing.

DOPS/(7,6)PC vesicle dispersions (4 mM) were then divided into 10 × 75 mm borosilicate culture tubes and diluted with either buffer alone or else buffer plus $CaCl_2$, to a final concentration of 2 mM lipid ± 20 mM Ca^{2+}. Typical sample volumes were 400–600 μL. The tubes were sealed under argon and placed in a KCl/ice bath (1/4 w/w) at −10 °C and incubated for 2–4 min. Samples were then nucleated to freeze by touching the tubes just above the meniscus with the tip of a pipe cleaner dipped in liquid N_2. The frozen samples were returned to the KCl/ice bath for an additional 2 min and then removed to thaw in a water bath. A total of 15 freeze–thaw cycles were performed. We note that samples of ≥0.70 mole fraction of DOPS initially showed aggregation and clumping in the presence of Ca^{2+}, but upon completion of the freeze–thaw process these samples appeared to be uniform, fine dispersions. Fluorescence measurements were made immediately following the last freeze–thaw cycle, since vesicles with a high PS content begin to aggregate noticeably in Ca^{2+} buffer after a period of 30–60 min.

Samples for EPR experiments were prepared from stock chloroform solutions in the same manner as described above, but with total lipid concentrations ranging from 2 to 40 mM. In all systems investigated, lipids were hydrated above the gel to liquid-crystal phase transition temperature. Samples containing Ca^{2+} were first hydrated without Ca^{2+} and then diluted into Ca^{2+}-containing buffer, followed by 15 freeze–thaw cycles to equilibrate the Ca^{2+}.

Fluorescence Spectroscopy. Fluorescence measurements were performed with a home-built spectrofluorometer [described in Caffrey and Feigenson (1981)] utilizing conventional 90° optics and equipped with double monochromators in both excitation and emission optics such that contributions from stray and scattered light were not detectable. Sample compartment temperature was 26–27 °C. The excitation/emission wavelengths used were 320/410 nm for samples containing tPnA-Me, 360/430 nm for DPH, and 385/470 nm for 12-AS-Me, 12-AS-PS, and 12-AS-PC. Nominal excitation and emission bandwidths were 2 and 16 nm, respectively, for fluorescence quenching experiments. For polarization measurements, the excitation bandwidth was 4 nm, but emission slits were removed due to the greatly decreased light transmission of the film polarizers used in the excitation and emission beams. The emission bandwidth was then approximately 40 nm.

Fluorescence polarization, p, was determined from measurements of fluorescence intensities emitted parallel (I_{VV}) and perpendicular (I_{VH}) to vertically polarized exciting light according to

$$p = \frac{\Delta I_{VV} - G\Delta I_{VH}}{\Delta I_{VV} + G\Delta I_{VH}} \quad (1)$$

where $\Delta I_{VV(VH)} = I^{sample}_{VV(VH)} - I^{blank}_{VV(VH)}$. Lipid blanks, which were prepared identically except for the addition of fluorophore, contributed background fluorescence of 1–10% of the sample fluorescence. The factor G represents a correction for the unequal transmission of differently polarized light and was determined according to Chen and Bowman (1965). For our instrument and experimental conditions, G ranged from 3.40 to 17.0, increasing with decreasing wavelength. Polarizer alignment was verified by use of fluorescein in alkaline glycerol, which yielded a value of $p = 0.446$ at 26 °C, in reasonable agreement with the value of 0.477 at 10 °C reported by Chen and Bowman (1965).

Fluorescence measurements were made by diluting 2 mM sample into acrylic cuvettes of 1-cm^2 cross-section (Sarstedt) containing the same buffer (10 mM Hepes and 100 mM KCl ± 20 mM Ca^{2+}, pH 7.0) to a final volume of 2 mL and lipid concentration of 100 μM. Preliminary experiments in which dilute fluorophore in sonicated vesicles was titrated with unlabeled DOPC or $Ca(PS)_2$ multilayers in the cuvette showed no increase in the fluorescence signal due to light scattering up to a lipid concentration of 250–300 μM (Feigenson, 1983). In fluorescence polarization experiments, 2 mM sample was diluted in the cuvette to a final lipid concentration of typically 150–300 μM. Further dilutions were performed in the cuvette, with polarization measurements obtained at four different lipid concentrations, the minimum being 50–75 μM. Depolarization of fluorescence due to light scattering in turbid solutions was never observed for DOPS samples. However, concentration-dependent p values were obtained for several probes in DPPC and $Ca(PS)_2$. For these samples, actual polarization was determined with the analysis of Teale (1969), as modified by Lentz et al. (1979), for membrane suspensions. Observed polarization values were converted to anisotropies [$r = 2p/(3 - p)$], and anisotropy was plotted against optical density (OD) at the exciting wavelength of the corresponding lipid blank, with extrapolation to zero OD to obtain the true anisotropy. A Beckman Model 25 spectrophotometer was used for OD measurements, which covered a range of 0.05–0.60. To confirm that optical density was a suitable indicator of sample turbidity, 90° light scattering data were obtained on successive dilutions of samples in the fluorescence cuvette, with the excitation and emission wavelengths set at the fluorophore emission wavelength. For the lipids DPPC, DOPS, and $Ca(PS)_2$, 90° light scattering at the emission wavelength was directly proportional to optical density of the corresponding lipid at the excitation wavelength over the range of lipid concentrations investigated. We note that $Ca(PS)_2$ dispersions gave the highest 90° light scattering signals while having the lowest OD values. Depolarization of fluorescence due to light scattering also was greatest in $Ca(PS)_2$.

Acrylic cuvettes were used for all fluorescence measurements, with polypropylene pipet tips (Eppendorf) used for all transfers, because vesicles containing high mole fractions of DOPS in the presence of excess Ca^{2+} stick to glass. Typical efficiency for a single transfer from a glass test tube or quartz cuvette was 60% (SD = 20%) for $Ca(PS)_2$, with transfer efficiency increasing with decreasing PS content, to, for example, 96% (SD = 3%) for samples with a mole fraction of PS = 0.8. In contrast, transfer efficiency between acrylic cuvettes was always approximately 100%. Transfer efficiency from the glass test tubes used for sample preparation was dependent on sample volume and concentration, as well as test-tube size. Because of the magnitude and variability of the losses, *for every fluorescence measurement, the lipid concentration in the cuvette was determined by phosphate analysis* of aliquots removed from the cuvettes directly following fluorescence measurements, according to a modification of the methods of Bartlett (1959) and Chen et al. (1956) as described by Kingsley and Feigenson (1979).

EPR Spectroscopy. For EPR measurements, 100-μL samples were placed in a flat quartz aqueous sample cell (Wilmad). Absorption derivative spectra were recorded on a Varian E-4 X-band spectrometer with 100-KHz field modulation, equipped with a variable-temperature accessory and interfaced to a DEC PDP-11/23 microcomputer. Instrument settings were normally as follows: modulation amplitude = 2 G, microwave power = 25 mW, filter time constant = 0.3 s, scan range = 100–200 G, and scan time = 2 min. Stored spectra were averages of three to nine scans. Prior to manipulation of experimental spectra, 1200-point stored spectra were smoothed once, by use of a nine-point quartic polynomial fit according to Savitzky and Golay (1964), and then integrated twice to obtain relative spin concentrations. An aqueous solution of the spin-label 2,2,6,6-tetramethylpiperidine-1-oxyl (TEMPO) was used to make field sweep calibrations (Knowles et al., 1976), from which hyperfine splittings were determined.

Quantitative estimates of the degree of motional restriction of the spin-labeled phospholipids were made by calculating the order parameter, S, which characterizes the average angular amplitude of motion of the molecular long axis with respect to the bilayer normal. S was determined according to

$$S = \frac{A_{\parallel} - (A_{\perp} + C)}{A_{zz} - (1/2)(A_{xx} + A_{yy})} \frac{a}{a'} \quad (2)$$

(Gaffney, 1976), where $A_{\parallel}$ and $A_{\perp}$ are, to a first approximation, equal to half the separation of the outer and inner hyperfine extrema, respectively, of the experimental spectra

(illustrated in Figure 3). A_{zz}, A_{xx}, and A_{yy} are the principal elements of the hyperfine tensor, C is a correction term allowing for the difference between the measured and true inner hyperfine splitting, and a/a' is a polarity correction term, with $a = (1/3)(A_{xx} + A_{yy} + A_{zz})$ and $a' = (1/3)[A_{\parallel} + 2(A_{\perp} + C)]$. In cases where $A_{\perp}$ could not be determined from the experimental spectra, the correction for possible polarity differences between the experimental sample and single-crystal environments was omitted; i.e., it was assumed that $a = a'$, such that S could be calculated according to

$$S = \frac{(3/2)[A_{\parallel} - (1/2)(A_{xx} + A_{yy})]}{A_{zz} - (1/2)(A_{xx} + A_{yy})} - \frac{1}{2} \qquad (3)$$

Implicit in these calculations are the assumptions of rapid rotational reorientation of the spin-label about the long axis of the probe molecule (i.e., correlation times faster than $\sim 3 \times 10^{-9}$ s), coincidence of the nitroxide z axis and the molecular long axis, and negligible spin–spin interactions.

Results

Nature of Ca^{2+}-Induced Gel Phase in Phosphatidylserine Multilayers

Concentration Dependence of Fluorescence Intensity of tPnA-Me, DPH, and 12-AS-Me. In order that fluorescence experiments be performed in the region of linear dependence of fluorescence on probe concentration, i.e., before the onset of "self-quenching", preliminary experiments were done with probe:lipid ratios between 1:2000 and 1:300 in DOPS ± Ca^{2+}. In DOPS, linearity was observed over the range of concentrations investigated with the exception of tPnA-Me, which showed a 10% decrease in fluorescence at 1:300 probe:lipid. However, in the presence of excess Ca^{2+}, fluorescence was decreased by 10% at approximately 1:500, 1:600, and 1:700 probe:lipid for tPnA-Me, 12-AS-Me, and DPH, respectively. Hence, all fluorescence quenching and polarization experiments were carried out at a probe:lipid ratio of 1:1000 for all fluorophores except tPnA-Me, for which a ratio of 1:500 was used to obtain sufficient fluorescence signal.

Spectral Characteristics and Steady-State Fluorescence Polarization of Single-Chain and Phospholipid Fluorescent Probes. Certain properties of probe fluorescence are sensitive to the local lipid environment being gel or fluid. The spectral characteristics and polarization values of the fluorescent probes in DOPS ± Ca^{2+} at 26 °C are summarized in Table I. For purposes of comparison, data are also shown for probes in multilamellar vesicles composed of gel-phase DPPC [T_t = 41.75 °C (Hinz & Sturtevant, 1972)].

For all fluorophores, the excitation maxima are unaffected by the physical state of the lipid (fluid or gel). For all of the 12-(9-anthroyloxy) fluorophores, the emission maximum is blue shifted 9 nm in DPPC, as reported by Bashford et al. (1976). In $Ca(PS)_2$, however, the only anthroyloxy label with a significant blue shift in its emission maximum is the labeled phosphatidylserine, 12-AS-PS, with a blue shift of 11 nm relative to DOPS.

A fluorescence intensity increase for tPnA-Me and for DPH is characteristic of gel-phase formation in DPPC [Sklar et al., 1977; B. Lentz in Shinitzky and Barenholz (1978); Table I]. In $Ca(PS)_2$ compared to fluid-phase DOPS, Table I shows a significant relative increase in tPnA-Me fluorescence, but little increase in DPH fluorescence. The AS probes show smaller but still significant increases in fluorescence intensity in gel-phase DPPC compared to fluid phase (Bashford et al., 1976; Table I). In $Ca(PS)_2$, compared with fluid DOPS, the fluorescence intensity of 12-AS-Me and 12-AS-PC is unchanged, whereas that of 12-AS-PS is markedly increased.

Table I: Fluorescence Properties of Probes in Multilamellar Lipid Vesicles at 26 °C

probe	vesicle composition	emission maximum (nm)	F/F_{DOPS}[a]	polarization (p)[b]
DPH	DOPS	431	1.00	0.129 ± 0.005
	$Ca(PS)_2$	431	1.1 ± 0.2	0.21 ± 0.01
	DPPC	431	1.5 ± 0.2	0.408 ± 0.004
tPnA-Me	DOPS	423	1.00	0.16 ± 0.01
	$Ca(PS)_2$	423	2.0 ± 0.2	0.27 ± 0.02
	DPPC	423	10 ± 1	0.33 ± 0.01
12-AS-Me	DOPS	452	1.00	0.09 ± 0.02
	$Ca(PS)_2$	449	1.0 ± 0.1	0.10 ± 0.02
	DPPC	443	1.1 ± 0.1	0.23 ± 0.01
12-AS-PC	DOPS	452	1.00	0.099 ± 0.002
	$Ca(PS)_2$	452	1.05 ± 0.05	0.13 ± 0.01
	DPPC	443	1.3 ± 0.2	0.20 ± 0.01
12-AS-PS	DOPS	452	1.00	0.09 ± 0.01
	$Ca(PS)_2$	441	2.0 ± 0.2	0.19 ± 0.02
	DPPC	443	1.2 ± 0.2	0.23 ± 0.01

[a] Intensity of probe fluorescence (F) in test lipid relative to that in DOPS (F_{DOPS}). [b] Values reported represent the average of several measurements made on each of triplicate samples, with error given by one standard deviation.

All of the fluorophores examined show increased polarization, indicative of slower or more restricted probe motion, in gel-phase DPPC relative to fluid-phase DOPS. In contrast, in $Ca(PS)_2$ each probe reflects a different degree of motional restriction imposed by the host lipid, as shown in Table I by the polarization values ranging between the values for fluid-phase DOPS and those for gel-phase DPPC. DPH, 12-AS-Me, and 12-AS-PC all exhibit a polarization in $Ca(PS)_2$ that is closer to that found in the fluid phase. 12-AS-PS and tPnA-Me, however, have polarizations in $Ca(PS)_2$ that are closer to DPPC gel-phase values. [We note that the value of $p = 0.33$ obtained for tPnA-Me in DPPC is somewhat lower than that reported by others (Sklar et al., 1979). The large grating correction factor of our instrument at 320/410 nm (G = 17.0) increases the uncertainty of our polarization measurements at these wavelengths.]

EPR Spectral Characteristics of Acyl Chain and Head Group Labeled Fatty Acid Ester Probes. The spin-label probes 12-DS-Me and TEMPO palmitate were used to investigate the $Ca(PS)_2$ phase. Figure 1a illustrates the effect of increasing probe concentration on the EPR spectrum of 12-DS-Me in the fluid lipid environment of DOPC at room temperature. As probe concentration increases, spin–spin interactions (dipolar and exchange) cause the spectral lines to broaden and eventually to merge. At a probe:lipid ratio of 1:200, no broadening is observed, and the spectrum reflects the low degree of ordering of the lipid acyl chains, in that the inner and outer hyperfine splittings, $A_{\perp}$ and $A_{\parallel}$ respectively, are not resolved. A similar spectrum is observed for 12-DS-Me in DMPS vesicles above the gel to liquid-crystal phase transition temperature of 36 °C (Cevc et al., 1981) (Figure 1c). Below T_t, however, the acyl chain order increases strongly with decreasing temperature, as indicated by the increase in $A_{\parallel}$ and the decrease in $A_{\perp}$. The spectrum for DMPS at 25 °C shows significant immobilization of the acyl chains in the gel phase. In contrast, in $Ca(PS)_2$ at 23 °C (Figure 1b), the spectrum of 12-DS-Me shows no evidence of probe immobilization but at a probe:lipid ratio of only 1:200 already displays significant concentration broadening. The nature of the concentration-dependent line broadening observed in $Ca(PS)_2$ is different from the line broadening for the fluid-phase lipid shown in

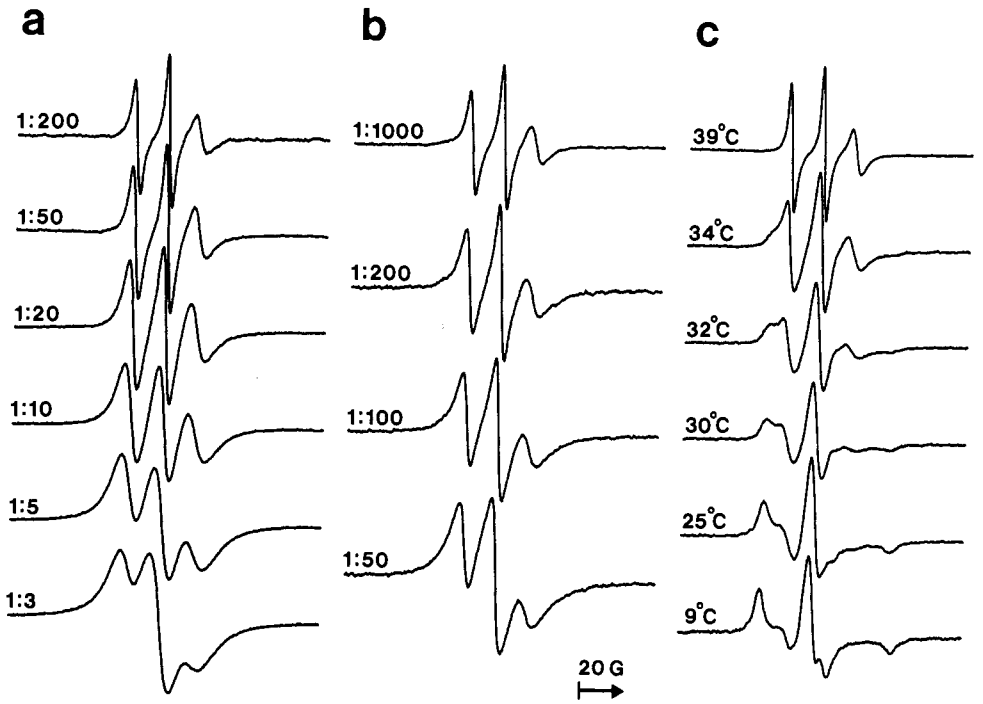

FIGURE 1: (a) Effect of increasing spin-label concentration on EPR spectra of 12-DS-Me in DOPC at 23 °C. Probe:lipid mole ratios are indicated. (b) Spectra of 12-DS-Me in DOPS in excess Ca^{2+} at 23 °C, with probe:lipid mole ratios indicated. (c) Effect of temperature on spectra of 12-DS-Me in DMPS, with probe:lipid = 1:200.

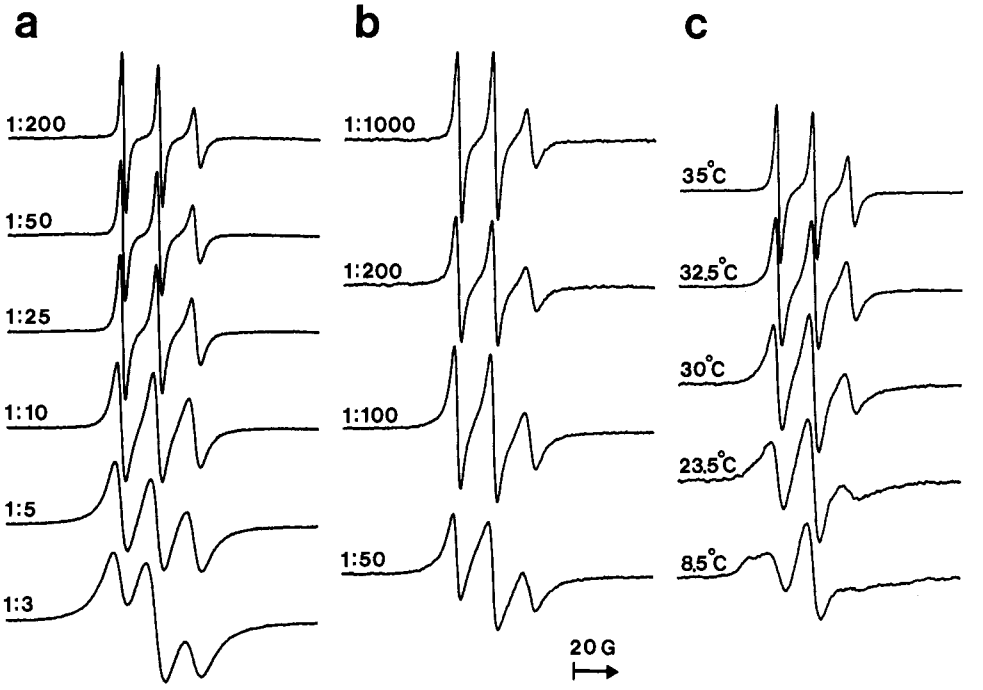

FIGURE 2: (a) Effect of increasing spin-label concentration on EPR spectra of TEMPO palmitate in DOPC at 23 °C. Probe:lipid mole ratios are indicated. (b) Spectra of TEMPO palmitate in DOPS in excess Ca^{2+} at 23 °C, with probe:lipid mole ratios indicated. (c) Effect of temperature on spectra of TEMPO palmitate in DMPS, with probe:lipid = 1:200.

Figure 1a. This difference is apparent in the relatively larger central peaks of Figure 1b. These spectra could be simulated reasonably well by spectral addition of normalized DOPC spectra of high and low spin concentration (data not shown). For example, the spectrum of 1:200 probe:lipid in DOPS in excess Ca^{2+} could be fit by a sum of mole fractions 0.25 and 0.75, respectively, of the spectra of 1:50 and 1:5 probe:lipid in DOPC, suggesting the presence in $Ca(PS)_2$ of clusters of 12-DS-Me of nonuniform probe concentration. The reasonable fit of such a simulation does not imply that the actual distribution of spin concentrations must be bimodal. In fact, the true distribution could not be uniquely determined by such a simple procedure. Whatever the distribution of the probe, however, its immediate lipid environment is fluid rather than gel.

TEMPO palmitate showed behavior similar to that of 12-DS-Me in each lipid environment, as Figure 2 illustrates. Because the nitroxide z axis of this probe is perpendicular rather than parallel to the long axis of the molecule as with the doxyl label, the z component of the hyperfine tensor is greatly reduced by rapid axial reorientation. However, there is evidence of motional restriction of TEMPO palmitate in

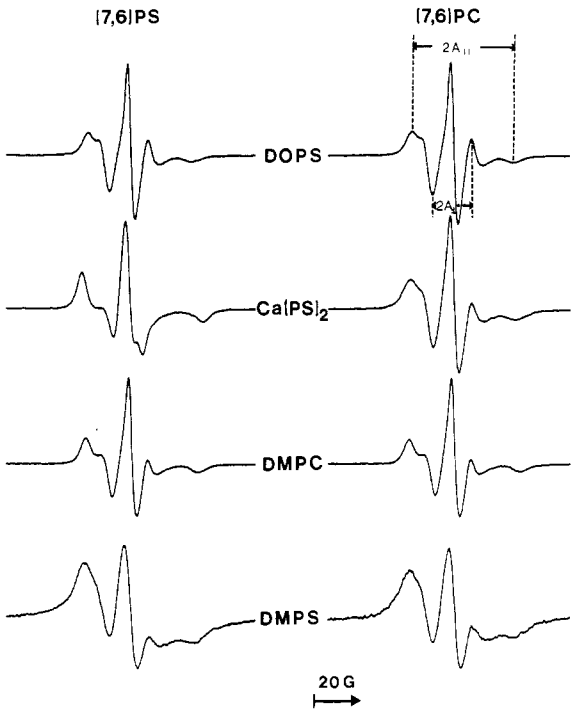

FIGURE 3: EPR spectra of 0.002 mole fraction of (7,6)PS and (7,6)PC in fluid-phase DOPS at 23 °C, DOPS in excess Ca^{2+} at 23 °C, gel-phase DMPC at 22 °C, and gel-phase DMPS at 23 °C.

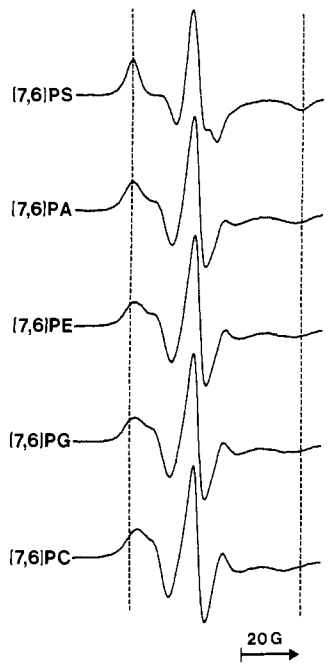

FIGURE 4: EPR spectra of 0.002 mole fraction of spin-labeled phospholipids in 40 mM DOPS after 15 freeze–thaw cycles in the presence of 40 mM Ca^{2+}, recorded at 23 °C.

gel-phase DMPS at room temperature (Figure 2c). In contrast, in $Ca(PS)_2$ (Figure 2b), no motional restriction is observed, and significant concentration broadening is apparent at 1:200 probe:lipid. As with 12-DS-Me, the spectral line broadening observed for TEMPO palmitate in $Ca(PS)_2$ is unlike that obtained in fluid-phase DOPC (Figure 2a). Probe clustering in $Ca(PS)_2$ is again observed, for example, with the spectrum of 1:100 probe:lipid in DOPS in excess Ca^{2+} fit reasonably well by a sum of mole fractions 0.2 and 0.8, respectively, of the spectra of 1:25 and 1:3 probe:lipid in DOPC.

EPR Spectra of Spin-Labeled Phospholipids: Comparison of $Ca(PS)_2$ Phase with Thermotropic Gel Phase. Spin-labeled phosphatidylserine and phosphatidylcholine were examined in four different lipid environments (Figure 3). (7,6)PS and (7,6)PC exhibit nearly identical spectra in DOPS at room temperature. In $Ca(PS)_2$, as compared to DOPS, the significant motional constraint of (7,6)PS is shown by the large increase in $A_{\parallel}$ and decrease in $A_{\perp}$. In contrast, the outer and inner hyperfine splittings for (7,6)PC in $Ca(PS)_2$ are virtually unchanged, although some concentration broadening is observed, as indicated by the broadened low-field peak and the downward displacement of the high-field hyperfine doublet. For comparison, spectra are also shown of (7,6)PS and (7,6)PC in gel-phase DMPC at 22 °C, just below the T_t of 23.7 °C (Hinz & Sturtevant, 1972). Both labeled lipids exhibit decreased motional freedom and no clustering in DMPC. In contrast, in gel-phase DMPS at 23 °C, (7,6)PC shows only slight motional restriction and considerable clustering. (7,6)PS also shows considerable clustering together with greater motional restriction than (7,6)PC in the same lipid.

The EPR spectra of five spin-labeled phospholipids in $Ca(PS)_2$ are compared in Figure 4. In DOPS without Ca^{2+}, all yield nearly identical spectra characteristic of a fluid phase [illustrated in Figure 3 for (7,6)PS and (7,6)PC]. However, the degree of order in $Ca(PS)_2$ is dependent on the head group of the labeled lipid. With the notable exception of (7,6)PC, all of the spin-labeled phospholipids exhibit increased motional restriction in $Ca(PS)_2$ relative to DOPS. The spectrum of (7,6)PS displays the largest increase in the separation of the outer hyperfine extrema, $2A_{\parallel}$, from approximately 50 G in DOPS to 59 G in $Ca(PS)_2$, followed by (7,6)PA, (7,6)PE, and lastly (7,6)PG, for which the outer hyperfine separations increase from 50 G in DOPS to 58, 57, and 56 G, respectively, in $Ca(PS)_2$.

Assuming rapid anisotropic motion of the spin-label about the long axis of the probe, increased ordering of the lipid acyl chains and, therefore, increased angular constraint of the spin-labels should be reflected in the EPR spectra by an increase in $A_{\parallel}$ accompanied by a decrease in $2A_{\perp}$ of equal magnitude, required by the rotational invariance of the trace of the hyperfine tensor (Seelig, 1970; Hubbell & McConnell, 1971). However, for (7,6)PA, (7,6)PE, and (7,6)PG in $Ca(PS)_2$, the observed increase in $A_{\parallel}$ is *not* accompanied by a significant decrease in $2A_{\perp}$. In each spectrum, the low-field minimum is shifted inward but the high-field maximum is shifted outward, such that the separation of the two inner extrema, which roughly approximates $2A_{\perp}$, decreases by only about 0.2 G relative to DOPS. This spectral feature is not an effect of spin–spin interactions, which were not observed until the mole fraction of probe in lipid reached 0.005 (data not shown).

The possibility that the observed spectra of (7,6)PA, (7,6)PE, and (7,6)PG in $Ca(PS)_2$ are actually composites of a rigid as well as a fluid component, resulting in anomalous measured values of $2A_{\perp}$, was investigated by spectral subtraction. The spectrum of each labeled phospholipid in DOPS (fluid component) was normalized to the observed $Ca(PS)_2$ spectrum and subtracted in various mole fractions to obtain the actual rigid component. For all three labeled lipids, spectral subtraction up to the point where distortions were observed, typically around 10 mol % fluid component, yielded little change in $A_{\parallel}$ and no significant decrease in $2A_{\perp}$, the position of the high-field maximum remaining unchanged. Similar results were obtained by subtracting various amounts of the spectrum of 0.002 mole fraction of (7,6)PC in $Ca(PS)_2$, which displays probe clustering, or the highly broadened spectrum of 0.7 mole fraction of (7,6)PC in DOPS. Thus, the

Table II: Order Parameters (S) for 0.002 Mole Fraction of Spin-Labeled Phospholipids in Multilamellar Vesicles[a]

	vesicle composition					
spin-label	DOPS	DMPC	DMPS	DPPC	DSPC	$Ca(PS)_2$
(7,6)PS	0.54	0.66	0.64	0.69	0.73	0.79
(7,6)PA	0.53	0.65	nd[b]	0.73	0.74	0.75
(7,6)PE	0.53	0.65	0.60	0.69	0.69	0.71
(7,6)PG	0.53	0.64	0.54	0.71	0.73	0.69
(7,6)PC	0.53	0.66	0.56	0.71	0.73	0.56

[a] All spectra were recorded at 23 °C with the exception of DMPC spectra, which were recorded at 22 °C, below the gel to liquid-crystal phase transition temperature. Order parameters were calculated by use of eq 3 (see text). [b] nd, not determined.

aberrant values of $2A_\perp$ observed in the spectra of (7,6)PA, (7,6)PE, and (7,6)PG in $Ca(PS)_2$ cannot be explained in terms of spin–spin interactions or the presence of an additional fluid component. We note that the spectra of (7,6)PS and (7,6)PE in gel-phase DMPS also exhibit an increase in $A_\parallel$ with no change in $2A_\perp$, relative to fluid-phase DOPS, although these spectra also contain an additional broad component [shown in Figure 3 for (7,6)PS].

The degree of motional restriction of the spin-labeled phospholipids in $Ca(PS)_2$ compared to thermotropic gel-phase lipids was estimated by calculating the order parameter, S, with eq 2 and 3. For all of the labeled phospholipids in DOPS, DMPC, DPPC, and DSPC, order parameters calculated from eq 2 did not differ significantly from those calculated from eq 3. Because of the anomalous behavior of the central region of the spectra of some of the labeled lipids in $Ca(PS)_2$ and DMPS, as well as the inability to measure $2A_\perp$ from the observed spectrum of (7,6)PS in $Ca(PS)_2$, S was determined from eq 3 for these spectra. Table II lists the order parameters calculated from eq 3 for the labeled phospholipids in DOPS ± Ca^{2+} as well as in several thermotropic gel-phase lipids at 22–23 °C. In fluid-phase DOPS, S is essentially the same for all (7,6)-labeled phospholipids and agrees well with the value of 0.55 reported by Gaffney and McConnell (1974) for (7,6)PC in egg PC. In thermotropic gel-phase PC, the order parameter for each labeled phospholipid increases with increasing host lipid T_t, from S = 0.64–0.66 in DMPC (T_t = 23.7 °C) to S = 0.69–0.74 in DSPC [T_t = 55.1 °C (Mason et al., 1981)]. Hubbell and McConnell (1971) report a value of S = 0.63 for (7,6)PC in DPPC at 23 °C, in reasonable agreement with our results. The increases in S in gel-phase DMPS (T_t = 36 °C) are considerably smaller than those in DMPC, which has a lower T_t. In $Ca(PS)_2$, unlike the thermotropic gel-phase lipids, the order parameters are strongly dependent on the head group of the labeled lipid, with $S_{PS} > S_{PA} > S_{PE} \approx S_{PG} > S_{PC}$. (7,6)PC exhibits no significant change in S in $Ca(PS)_2$ relative to DOPS.

The spectra of all spin-labeled phospholipids in DMPS, DPPC, and DSPC contained a broad feature indicative of a high spin concentration component, which was reduced significantly when the mole fraction of spin-label was decreased from 0.002 to 0.001. This apparent clustering was not an artifact of sample preparation, because samples prepared by lyophilization from benzene rather than by drying from chloroform yielded similar spectra. (We note that the fatty acid ester probes 12-DS-Me and TEMPO palmitate exhibited gel-phase spectra in DMPS and DPPC at 23 °C with no evidence of probe clustering in either lipid.)

Ca^{2+}-Induced Phase Separation in PS/PC Mixtures

Calculation of Phase Boundaries. The effect of Ca^{2+} on multilamellar vesicles composed of phosphatidylserine and phosphatidylcholine was examined in two PS/PC systems,

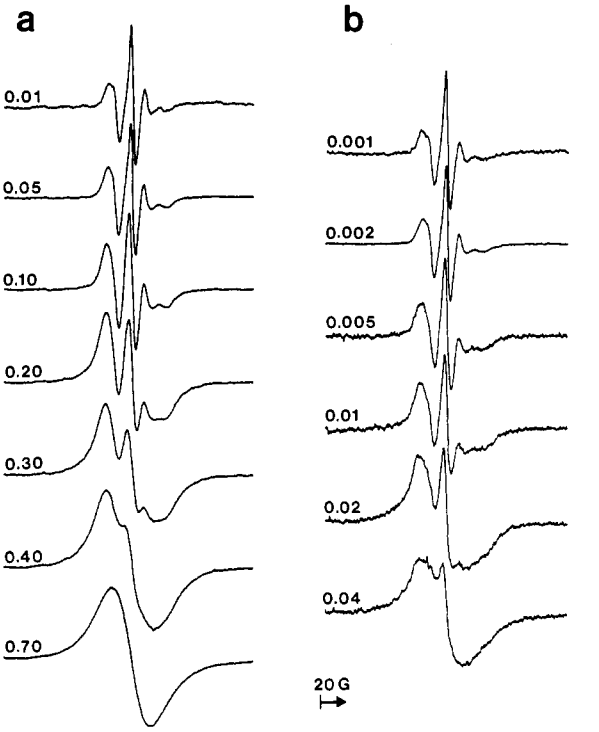

FIGURE 5: Effect of Ca^{2+} on EPR spectra of DOPS/(7,6)PC multilamellar vesicles of varying spin-label concentration. Spectra were recorded at 23 °C after 15 freeze–thaw cycles in (a) buffer only or (b) buffer with excess Ca^{2+}. The mole fractions of (7,6)PC in the dispersions are indicated in the figure.

DOPS/(7,6)PC and DOPS/DOPC. EPR spectra from vesicles composed of DOPS and (7,6)PC (Figure 5a) begin to exhibit spin–spin interactions at about 0.02 mole fraction of (7,6)PC. Spectral broadening increases with increasing spin concentration until a single broad line is observed at 0.55–0.60 mole fraction of (7,6)PC. In the presence of excess Ca^{2+}, a dramatic change takes place (Figure 5b). At a mole fraction of (7,6)PC of as little as 0.001–0.002, there is already evidence of concentration broadening, yet no evidence of increased motional restriction. As the amount of (7,6)PC increases, the spectra are broadened to a much greater degree than those of the same spin-label concentration without Ca^{2+}. The spectra of Figure 5b could be simulated reasonably well as composites of a dilute (7,6)PC spectrum and a broadened (7,6)PC-rich spectrum, suggesting Ca^{2+}-induced phase separation into a DOPS phase containing only a trace of (7,6)PC and into a (7,6)PC-rich phase. Thus, the solidus boundary must be close in composition to 0.00 mole fraction of (7,6)PC in $Ca(PS)_2$, because the two-phase region is already manifest at a few mole percent of (7,6)PC. The liquidus boundary is difficult to establish because there is so little (7,6)PC in the solid phase that EPR sensitivity is low for detecting the appearance of a small amount of this phase. However, the liquidus boundary can be estimated to be at about 0.5–0.6 mole fraction of (7,6)PC, the label concentration beyond which the EPR spectra for DOPS/(7,6)PC with and without Ca^{2+} are superimposable (data not shown).

(7,6)PS was used to confirm the existence of two well-defined phases in DOPS/DOPC vesicles in the presence of excess Ca^{2+} (Figure 6). The probe:lipid mole ratio was kept constant at 1:200, with EPR spectra obtained over a range of DOPS/DOPC compositions. Stored spectra were scaled to the same spin concentration, and the observed spectra for [DOPS] = 0.35–0.95 were fit, by the method of least squares, as composites of the [DOPS] = 1.00 (gel) and [DOPS] = 0.00 (fluid) spectra. The excellent agreement between the observed

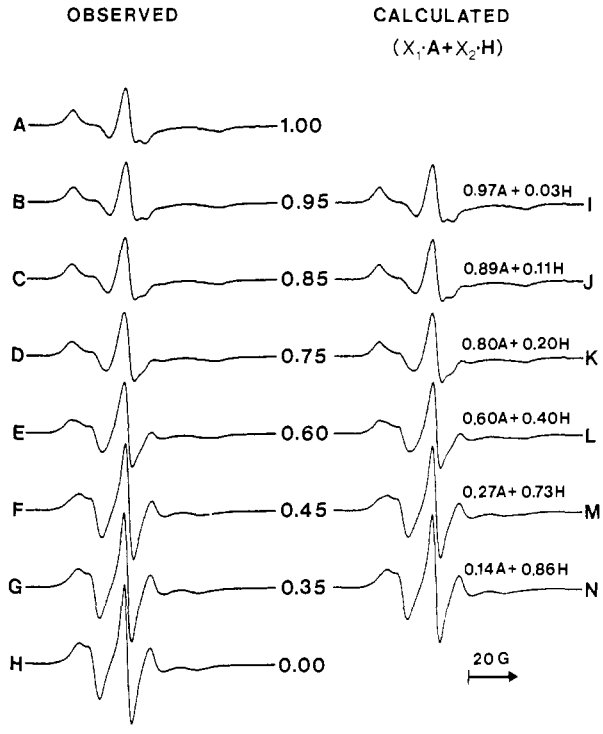

FIGURE 6: EPR spectra of (7,6)PS in DOPS/DOPC in excess Ca^{2+} at 23 °C, with mole fraction of DOPS indicated. Probe:lipid mole ratio = 1:200. (A–H) Experimental spectra that have been smoothed, and scaled to the same spin concentration. (I–N) Calculated as composites of mole fractions X_1 and X_2 of spectra A and H, respectively.

and composite spectra supports the assumption of two coexisting phases, since the EPR spectrum of a spin-labeled probe molecule in a two-phase region should be a superposition of the EPR spectrum of the probe in a sample of the solidus boundary composition plus a spectrum of the probe in a sample of the liquidus boundary composition. The phase boundaries can be estimated from changes in the EPR spectra of (7,6)PS as the PS/PC composition changes. The change in the central region of the spectrum already observed at 0.95 mole fraction of DOPS (spectrum B of Figure 6) indicates that the solidus boundary is located near 1.00 mole fraction of DOPS. The minimal differences between the 0.35 and 0.00 mole fraction of DOPS spectra (spectra G and H of Figure 6) indicate that the liquidus boundary is located in the vicinity of 0.3 mole fraction of DOPS. [We note that because the EPR spectra of (7,6)PS in *fluid-phase* DOPS (Figure 3) and DOPC (spectrum H of Figure 6) are identical, spectrum H is an acceptable choice for the fluid basis spectrum used in the spectral simulations, even though its lipid composition is not that of the liquidus boundary.]

The liquidus boundary for each of the two PS/PC systems investigated was more accurately identified by X-ray diffraction (M. Caffrey, unpublished experiments). For DOPS/(7,6)PC in excess Ca^{2+} at 23.5 °C, the liquidus boundary is located at $[7,6)PC]_{LC}$ = 0.55–0.60. For DOPS/DOPC, $[DOPC]_{LC}$ = 0.65–0.70. The X-ray results for both PS/PC systems are in reasonable agreement with the EPR observations.

Partitioning of Probe Molecules in PS/PC Vesicles in the Presence of Ca^{2+}. If the phase boundaries are known for a mixture of two unlabeled phospholipids, then the partition behavior of a spin-labeled probe molecule can be determined from simulations of the observed EPR spectra in the two-phase region, provided that the probe has significant solubility in each phase. As Figure 6 illustrates for DOPS/DOPC in excess Ca^{2+} at 23 °C, (7,6)PS is soluble in both the gel phase (spectrum A) and the fluid liquid-crystal phase (spectrum H). Partitioning of (7,6)PS in the two-phase region can be expressed in terms of a concentration ratio, $R_{LC/G}$, for the probe between phases and is defined as

$$R_{LC/G} = \frac{(\text{probe})_{LC}/[LC]}{(\text{probe})_{G}/[G]} \quad (4)$$

where $(\text{probe})_{LC(G)}$ = the fraction of all probe molecules in the liquid-crystal (gel) phase and [G]/[LC] = the mole ratio of lipids in the gel phase to lipids in the liquid-crystal phase. From the lever arm rule for phase diagrams (Moore, 1962)

$$\frac{[G]}{[LC]} = \frac{[\text{DOPS}] - [\text{DOPS}]_{LC}}{[\text{DOPS}]_{G} - [\text{DOPS}]} \quad (5)$$

where $[\text{DOPS}]_{LC(G)}$ = the mole fraction of liquid-crystal (gel) phase that is composed of DOPS, at the boundary of the two-phase region, and [DOPS] = the overall mole fraction of DOPS in the vesicles. The ratio $(\text{probe})_{LC}/(\text{probe})_{G}$ is found from the spectral simulations (spectra I–N of Figure 6) and is equal to X_2/X_1. Thus, from eq 4 and 5, the ratio of the probe concentration in the liquid-crystal phase to that in the gel phase, $R_{LC/G}$, can be calculated for each spectrum in the two-phase region according to

$$R_{LC/G} = \frac{X_2}{X_1}\frac{[\text{DOPS}] - [\text{DOPS}]_{LC}}{[\text{DOPS}]_{G} - [\text{DOPS}]} \quad (6)$$

Using $[\text{DOPS}]_{G}$ = 1.00 and $[\text{DOPS}]_{LC}$ = 0.32, concentration ratios were calculated from eq 6 with data from 13 spectral simulations, including those shown in Figure 6, yielding an average value of $R_{LC/G}$ = 0.45 (SD = 0.09) for (7,6)PS in DOPS/DOPC in excess Ca^{2+} at 23 °C, indicating probe partitioning into the $Ca(PS)_2$ gel phase.

The behavior of the fluorescent membrane probes in PS/PC vesicles in excess Ca^2 was examined with a method developed in this laboratory whereby the local lipid environment of a membrane-bound fluorophore can be determined from the contact quenching of fluorescence by nitroxide spin-labeled phospholipids (London & Feigenson, 1981a). Fluorescence is measured as the mole fraction of spin-labeled lipid in a binary lipid mixture is varied from 0 to 1, generating a fluorescence quenching curve. In a one-phase fluid system, the quenching curve reflects the random distribution of spin-labeled and unlabeled phospholipids around the fluorophore. Ca^{2+}-induced lipid phase separation yields a quenching curve that reflects, in the two-phase region, the partitioning of the fluorophore between the two coexisting phases. The lipid composition of each phase determines the quantum yield of fluorescence for the fluorophore in that phase.

Fluorescence quenching curves for tPnA-Me, DPH, 12-AS-Me, 12-AS-PC, and 12-AS-PS in DOPS/(7,6)PC ± Ca^{2+} are shown in Figure 7. In the presence of excess Ca^{2+}, all five probes exhibit significant changes in their fluorescence behavior. If these changes are described by a partitioning of the fluorophore between a Ca^{2+}-induced (7,6)PC-depleted gel phase and a (7,6)PC-rich liquid-crystal phase, and knowing the phase boundaries for DOPS/(7,6)PC in excess Ca^{2+}, we can determine the ratio of the fluorophore concentration in the liquid-crystal phase to that in the gel phase, $R_{LC/G}$, from the fluorescence quenching data according to

$$F = (F)_{LC} + \frac{[G]}{R_{LC/G}(1 + [G]) + [G]}[(F)_{G} - (F)_{LC}] \quad (7)$$

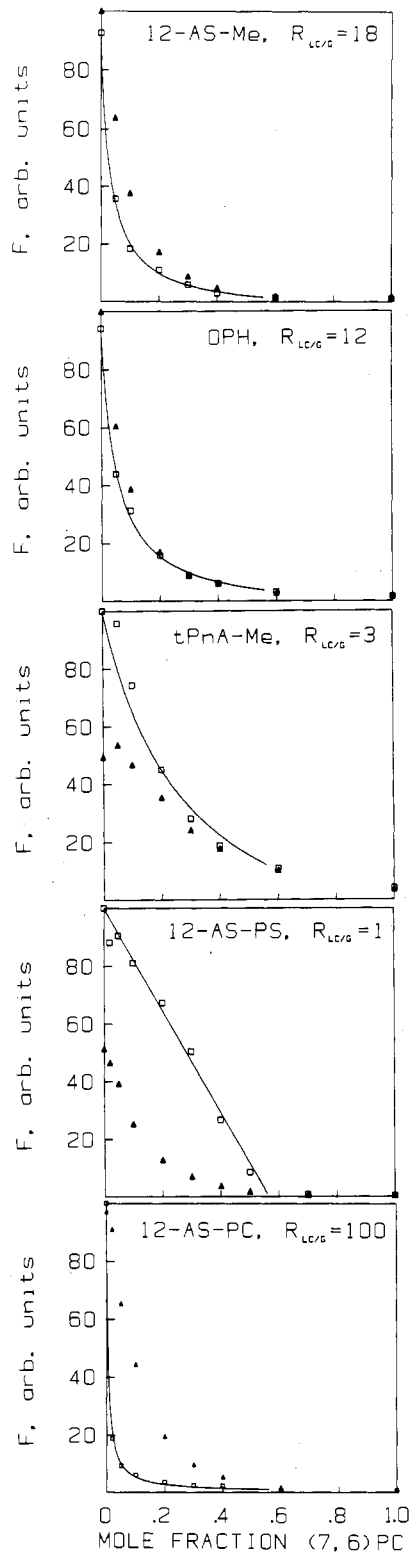

FIGURE 7: Fluorescence quenching of various fluorophores in multilamellar vesicles composed of DOPS/(7,6)PC. The abscissa is the mole fraction of (7,6)PC in the vesicles, and the ordinate is the observed or calculated fluorescence. Observed probe fluorescence, F, in 100 μM lipid with (□) or without (▲) 20 mM Ca^{2+}. Symbol height represents the range of triplicate F measurements. Solid lines are theoretical curves calculated by use of eq 7 (text) for the indicated values of the concentration ratio, $R_{LC/G}$, of fluorophore in a liquid-crystal phase of (7,6)PC mole fraction of 0.56 to that in a rigid phase of (7,6)PC mole fraction of 0.00. Mole ratio of probe:lipid is 1:500 for tPnA-Me and 1:1000 for all other fluorophores.

where F = measured or calculated fluorescence intensity, $(F)_{G(LC)}$ = fluorescence in a membrane of the composition at the gel (or liquid-crystal) phase boundary, and

$$[G] = \frac{[(7,6)PC]_{LC} - [(7,6)PC]}{[(7,6)PC]_{LC} - [(7,6)PC]_G}$$

(London & Feigenson, 1981b).[2] $R_{LC/G}$ is determined by fitting the experimental data to theoretical curves of F vs. [(7,6)PC] in the two-phase region calculated from eq 7 with $[(7,6)PC]_{LC}$ = 0.56 and $[(7,6)PC]_G$ = 0.00. For $R_{LC/G}$ = 1, fluorescence quenching would be linear with [(7,6)PC]. $R_{LC/G}$ > 1 would indicate fluorophore partitioning into the (7,6)-PC-rich fluid liquid-crystal phase. Outside the two-phase region, i.e., for [(7,6)PC] > 0.56, the quenching curves for fluorophore in DOPS/(7,6)PC ± Ca^{2+} are superimposable. As Figure 7 illustrates, the fluorescence data in DOPS/(7,6)PC in excess Ca^{2+} are best fit with $R_{LC/G}$ = 3 ± 1 for tPnA-Me, $R_{LC/G}$ = 12 ± 1 for DPH, $R_{LC/G}$ = 18 ± 2 for 12-AS-Me, $R_{LC/G}$ = 100 ± 20 for 12-AS-PC, and $R_{LC/G}$ = 1.0 ± 0.2 for 12-AS-PS.

Discussion

In this study, we have utilized fluorescence and EPR spectroscopy to examine the effects of Ca^{2+} binding to phosphatidylserine in multilamellar vesicles composed of DOPS or mixtures of DOPS/DOPC or DOPS/(7,6)PC. Because steady-state measurements have been used throughout, any distribution of probe environments results in ensemble averaged (fluorescence) or superimposed (EPR) spectral measurements. Nonetheless, certain conclusions are clear. In DOPS vesicles, the presence of Ca^{2+} results in the formation of a rigid $Ca(PS)_2$ phase. In PS/PC mixtures at room temperature, Ca^{2+} induces lipid phase separation into a rigid PS phase that excludes PC and a PC-rich fluid phase. The boundaries of the phase coexistence region of two different PS/PC systems have been determined. EPR spectroscopy was used to identify the solidus boundary in each system but was not sensitive to the appearance of gel phase in DOPS/(7,6)PC and, therefore, not useful for locating the liquidus boundary in this system. X-ray diffraction, which is sensitive to the onset of gel phase (Caffrey & Feigenson, 1984), was used to accurately identify the liquidus boundaries. The two methods yield $[PS]_G$ = 1.00 and $[PS]_{LC}$ = 0.30–0.35 for DOPS/DOPC and $[PS]_G$ = 1.00 and $[PS]_{LC}$ = 0.40–0.45 for DOPS/(7,6)PC in excess Ca^{2+} at 23 °C. These results are in qualitative agreement with those reported for BBPS/egg PC multilayers bound to a filter support in excess Ca^{2+} (Tokutomi et al., 1981).

For each of the gel phases examined here—DMPC, DPPC, DSPC, DMPS, and $Ca(PS)_2$—a particular pattern of spectroscopic behavior for incorporated probes is observed. In DMPC at 22 °C, just below the gel to liquid-crystal phase transition temperature, the EPR spectra of the five spin-labeled phospholipids reveal significantly increased angular constraint

[2] The analysis developed by London and Feigenson describes the ratio of fluorophore concentration in the liquid-crystal phase to that in the gel phase as a partition coefficient, K_p. To use a *partition coefficient* for characterizing the behavior of a probe molecule in the presence of coexisting lipid phases is to describe the behavior as being at *equilibrium*; i.e., the chemical potential of the probe molecule is the same in both phases. However, neither we nor others have tested this equilibrium assumption for coexisting lipid solid and fluid phases. It is possible that the observed ratio of concentrations of the probe in coexisting phases is influenced by kinetic effects; i.e., the probe is trapped within the solid phase, diffusing so slowly that the equilibrium distribution between solid and fluid phases is not reached during the experiment. Because of this uncertainty, we use the term "concentration ratio" for characterizing the behavior of a probe molecule in the presence of coexisting solid and fluid lipid phases. If equilibrium obtains, $R_{LC/G} = K_P$.

of probe motion, shown by the increased order parameters, no broad component indicative of probe clustering, and no fluid component that would suggest a heterogeneity of probe sites.

In gel-phase DPPC at 23 °C, all five fluorescent probes, as well as all seven spin-label probes, exhibit more restricted and/or slower molecular motion than is observed in fluid-phase DOPS. Motional restriction comparable to that observed in gel-phase DPPC for the five spin-labeled phospholipids is also observed in gel-phase DSPC at the same temperature. In both DPPC and DSPC, the spin-labeled phospholipids also show a broad EPR spectral component, indicating probe clustering.

In gel-phase DMPS at 23 °C, the EPR spectra of the spin-label probes 12-DS-Me and TEMPO palmitate reveal considerable probe immobilization with no evidence of probe clustering. The five spin-labeled phospholipids, however, exhibit less motional restriction than would be expected on the basis of the T_t of 36 °C, with order parameters less than those found in DMPC at 22 °C. In addition to a broad component observed in the spectra of all of the spin-labeled phospholipids in gel-phase DMPS, the spectra of (7,6)PS and (7,6)PE exhibit an increase in $A_{\parallel}$ relative to fluid-phase DOPS with no change in $2A_{\perp}$, indicating that these spectra cannot be explained simply in terms of rapid anisotropic motion of the spin-labels within a more restricted volume. Motional effects, e.g., a significant decrease in the rate of rotation of the spin-label about the long axis of the probe molecule, and/or conformational changes, e.g., kinks in the acyl chain such that the nitroxide z axis is no longer parallel to the molecular long axis, might be responsible for the observed anomalies in these spectra. Examples of such motional or conformational behavior for spin-labeled PC have been reported. Marsh (1980), using saturation transfer EPR, reports effective correlation times for long axis rotation of a spin-labeled PC in gel-phase DPPC and DMPE at 25 °C of 10^{-4} s. Lange et al. (1985) report long axis rotational correlation times of 10^{-7} s for a spin-labeled PC in oriented bilayers of DMPC at 22 °C as well as a distribution of tilt angles of the lipid chains and trans–gauche isomerization in the slow-motion regime.

Fluorescent-labeled and spin-labeled phosphatidylserine probes are informative about the nature of the $Ca(PS)_2$ phase. The spectral characteristics and polarization values of 12-AS-PS in $Ca(PS)_2$ indicate a high degree of order in the lipid acyl chains in the presence of Ca^{2+}. Although we have not attempted to measure fluorescence decay times, the motional constraint of 12-AS-PS in $Ca(PS)_2$ is likely to be very great, because the observed increased fluorescence intensity corresponds to an increased fluorescence decay time, which in itself would decrease polarization unless motion were restricted. The EPR spectrum of (7,6)PS in $Ca(PS)_2$ also indicates strongly constrained motion of the probe relative to the bilayer normal as reflected in the high value of $\sim$0.8 for the order parameter.

The behavior of phospholipid probes in $Ca(PS)_2$ appears to be dominated by the interaction of Ca^{2+} with the lipid head group. 12-AS-PS, (7,6)PS, (7,6)PA, (7,6)PE, and (7,6)PG exhibit motional restriction comparable to that observed in thermotropic gel-phase lipids 10–30 °C below T_t (Tables I and II), with (7,6)PS displaying even greater immobilization. In the case of the spin-labeled phospholipids (7,6)PA, (7,6)PE, and (7,6)PG in $Ca(PS)_2$, anomalous behavior of the central region of the EPR spectra is observed that is similar to that observed for (7,6)PS and (7,6)PE in gel-phase DMPS. The spectral features cannot be attributed to spin–spin interactions, nor can they be explained in terms of simple two-component spectra. These labeled lipids may occupy sites in the $Ca(PS)_2$ lattice in which the tight packing of the neighboring acyl chains imposes a degree of motional restriction that is dependent on the degree to which the probe lipid head group perturbs the lattice, and they may also occupy defect regions in the lattice, for example, at domain boundaries, where less ordered lipid packing results in greater motional freedom. The actual distribution of orientations of the probe molecules and their rates of motion cannot be determined from the experimental spectra, and the order parameters listed in Table II, which are based on the maximum hyperfine splitting, at best represent an upper bound on the degree of motional restriction. Computer simulations are planned to extract information on the ordering and dynamics of these probes.

The phosphatidylcholine probes, 12-AS-PC and (7,6)PC, with no net charge and relatively bulky head groups show no significant motional restriction in $Ca(PS)_2$, implying either that they are completely excluded from the gel phase or that they disrupt the acyl chain packing of the surrounding lipid molecules sufficiently to create fluid microdomains. Although the details of the local environment of the (7,6)PC in $Ca(PS)_2$ cannot be uniquely determined from the EPR spectra, it is clear that at the lowest probe concentrations true phase separation has not yet occurred, because the (7,6)PC concentration of 56 mol % in the equilibrium PS/PC fluid phase in the presence of Ca^{2+} would give rise to an EPR spectrum consisting of a single broad line (see Figure 5). [We note that the polarization of 12-AS-PC in DOPS does increase in the presence of Ca^{2+}, though to a lesser extent than that of 12-AS-PS. However, the fluorescence intensity and position of the emission maximum remain unchanged, indicative of a fluid environment.]

Of the single-chain fluorescent probes, DPH, 12-AS-Me, and tPnA-Me, and spin-label probes, 12-DS-Me and TEMPO palmitate, examined in $Ca(PS)_2$, only tPnA-Me, with its greatly increased fluorescence intensity and polarization, exhibits significant motional restriction. The fluorescence properties of DPH and 12-AS-Me in $Ca(PS)_2$ are essentially the same as in DOPS, and 12-DS-Me and TEMPO palmitate exhibit fluid EPR spectra in both DOPS and $Ca(PS)_2$. In addition, all five probes show aggregation in $Ca(PS)_2$ at considerably lower probe:lipid ratios than in fluid-phase DOPS, the fluorescent probes exhibiting self-quenching in $Ca(PS)_2$ for probe:lipid ratios as low as 1:700 and the spin-labels exhibiting spectral broadening indicative of probe clustering. The tPnA-Me is certainly the least perturbing of the five probes, since it is a linear polyene with no added ring structure. However, even this probe shows less motional restriction in $Ca(PS)_2$ than in gel-phase DPPC, according to its polarization and fluorescence intensity. A more complete description of the motional state of the fluorescence probes would involve time-resolved measurements in order to estimate motional correlation times and to characterize possible multiple probe environments (Blatt et al., 1983; Parasassi et al., 1984a,b; Barrow & Lentz, 1985).

In DOPS/(7,6)PC vesicles in the presence of excess Ca^{2+}, 12-AS-Me, DPH, and tPnA-Me favor the fluid phase, with concentration ratios $R_{LC/G}$ of 18 ± 2, 12 ± 1, and 3 ± 1, respectively. 12-(9-Anthroyloxy)stearic acid has been reported to partition strongly into the fluid phase of thermally induced phase-separated DPPC/DLPC membranes (Bashford et al., 1976), while tPnA-Me has a partition coefficient of 4 ± 1 in favor of the *gel* phase in DPPC/PDPC mixtures (Sklar et al., 1979). DPH partitions equally (K_p = 1) between thermally induced gel and fluid phases of DPPC/DMPC (Lentz et al., 1976) or DPPC/(7,6)PC (London & Feigenson, 1981b). A value of K_p = 1 has also been found for DPH in egg PC/

(7,6)PA vesicles in the presence of excess cadmium (Feigenson, 1983). Our results for probe partitioning in PS/PC multilayers in excess Ca^{2+} support the fluorescence and EPR observations in pure PS that the $Ca(PS)_2$ gel phase is highly ordered and exlcudes probe molecules to a greater degree than do thermotropic gel-phase lipids (or Cd^{2+}-induced gel-phase PA). For the limited series of three probes examined, partitioning into the fluid phase would appear to be proportional to probe "bulkiness", the order of partitioning being 12-AS-Me > DPH > tPnA-Me.

Fluorescence quenching measurements in DOPS/(7,6)PC in excess Ca^{2+} yield concentration ratios of 1.0 ± 0.2 for 12-AS-PS and 100 ± 20 for 12-AS-PC. The strong partitioning of 12-AS-PC into the fluid phase confirms the dramatic EPR results illustrated in Figure 5b, namely, the formation in the presence of Ca^{2+} of a $Ca(PS)_2$ phase that excludes PC. The fact that 12-AS-PS partitions about equally between the two phases ($R_{LC/G} = 1$) rather than mimicking the unlabeled DOPS exactly is evidence that the 9-anthroyloxy probe moiety alters the behavior of 12-AS-PS compared to DOPS. [If 12-AS-PS behaved exactly like DOPS, then its location would follow the volume of each phase *weighted* by the mole fraction of PS in each phase, resulting in a quenching curve that lies above the $R_{LC/G} = 1$ curve.] In addition, the fact that 12-AS-PS does not partition strongly into the fluid phase makes it useful for detecting the locations of the lipid phase boundaries, since the fluorescence quenching curve in the presence of Ca^{2+} intersects the curve in the absence of Ca^{2+} at clearly defined locations, thereby locating the compositions of the phase boundaries. As Figure 7 illustrates, the curves intersect at approximately [(7,6)PC] = 0.00 and 0.55, in good agreement with the EPR and X-ray results.

EPR spectra of (7,6)PS in DOPS/DOPC in excess Ca^{2+} in the phase coexistence region can be fit as composites of a gel- and a fluid-phase component to yield the distribution of the spin-label between gel and fluid lipid phases, with the result $R_{LC/G} = 0.45$. In principle, this method can be used to determine the ratio of probe concentration in the liquid-crystal phase to that in the gel phase, $R_{LC/G}$, for any spin-label probe in any lipid mixture in which two phases are present, provided that the probe has significant solubility in each phase and that the boundaries of the two-phase region are known. Investigations of the partition behavior of other spin-labeled phospholipids as well as fatty acid derivatives in PS/PC mixtures in the presence of Ca^{2+} are planned.

We conclude that the $Ca(PS)_2$ rigid phase has a pronounced characteristic, as compared to other phospholipid gel phases, of excluding certain other, non-PS, membrane-bound small organic molecules. We conjecture that this "exclusion character" arises because the great stability of the $Ca(PS)_2$ structure depends upon strict stereochemical requirements for the head group atoms and for at least a portion of the lipid acyl chains. The molecules that are excluded from the $Ca(PS)_2$ structure might act as impurities in the $Ca(PS)_2$ lattice that disrupt the lipid packing in the immediate vicinity, creating the fluid lipid environment indicated in the EPR spectra and in the fluorescence behavior. Alternatively, the probes may be forced out of the orderly domains of the $Ca(PS)_2$ lattice and into defect regions, perhaps at domain boundaries. As probe concentration in the vesicles is increased, the probe molecules could congregate in these fluid regions and produce broadened EPR spectra or self-quenching of fluorescence.

Because of the possibility that $Ca(PS)_2$ could form at Ca^{2+} concentrations that are found inside cells (Feigenson, 1986), we are especially interested in which kinds of membrane-bound molecules are, and which are not, excluded from $Ca(PS)_2$. We are also looking for which lipids promote, and which inhibit, the formation of $Ca(PS)_2$.

ACKNOWLEDGMENTS

We gratefully acknowledge the technical assistance of Mark Yeager in synthesizing the (7,6)PS and providing the computer programs used for spectral analysis and plotting. We thank Martin Caffrey for performing the X-ray diffraction measurements and Rajindra Aneja for synthesizing the 12-AS-PS. We also thank M. Caffrey and M. Yeager for helpful discussions and Ellen Patterson for typing the manuscript.

Registry No. DOPS, 70614-14-1; DMPS, 64023-32-1; DOPC, 4235-95-4; DMPC, 18194-24-6; DPPC, 63-89-8; DSPC, 816-94-4.

REFERENCES

Barrow, D. A., & Lentz, B. R. (1985) *Biophys. J. 48*, 221–234.
Bartlett, G. R. (1959) *J. Biol. Chem. 234*, 466–468.
Bashford, C. L., Morgan, C. R., & Radda, G. K. (1976) *Biochim. Biophys. Acta 426*, 157–172.
Bentz, J., Düzgünes, N., & Nir, S. (1983) *Biochemistry 22*, 3320–3330.
Blatt, E., Sawyer, W. H., & Ghiggino, K. P. (1983) *Aust. J. Chem. 36*, 1079–1086.
Boggs, J. M., Wood, D. D., Moscarello, M. A., & Papahadjopoulos, D. (1977) *Biochemistry 16*, 2325–2329.
Browning, J., & Seelig, J. (1980) *Biochemistry 19*, 1262–1270.
Caffrey, M., & Feigenson, G. W. (1981) *Biochemistry 20*, 1949–1961.
Caffrey, M., & Feigenson, G. W. (1984) *Biochemistry 23*, 323–331.
Cevc, G., Watts, A., & Marsh, D. (1981) *Biochemistry 20*, 4955–4965.
Chen, P. S., Toribara, T. Y., & Warner, H. (1956) *Anal. Chem. 28*, 1756–1758.
Chen, R. F., & Bowman, R. L. (1965) *Science (Washington, D.C.) 147*, 729–732.
Comfurius, P., & Zwaal, R. F. A. (1977) *Biochim. Biophys. Acta 488*, 36–42.
Düzgünes, N., Paiement, J., Freeman, K. B., Lopez, N. G., Wilschut, J., & Papahadjopoulos, D. (1984) *Biochemistry 23*, 3486–3494.
Feigenson, G. W. (1983) *Biochemistry 22*, 3106–3112.
Feigenson, G. W. (1986) *Biochemistry 25*, 5819–5825.
Gaffney, B. J. (1976) in *Spin Labeling: Theory and Applications* (Berliner, L. J., Ed.) pp 567–571, Academic, New York.
Gaffney, B. J., & McConnell, H. M. (1974) *J. Magn. Reson. 16*, 1–28.
Hauser, H., & Shipley, G. G. (1984) *Biochemistry 23*, 34–41.
Hinz, H. J., & Sturtevant, J. M. (1972) *J. Biol. Chem. 247*, 6071–6075.
Hoekstra, D. (1982) *Biochemistry 21*, 1055–1061.
Hubbell, W. L., & McConnell, H. M. (1971) *J. Am. Chem. Soc. 93*, 314–326.
Hui, S. W., Boni, L. T., Stewart, T. P., & Isac, T. (1983) *Biochemistry 22*, 3511–3516.
Kingsley, P. B., & Feigenson, G. W. (1979) *Chem. Phys. Lipids 24*, 135–147.
Knowles, P. F., Marsh, D., & Rattle, H. W. E. (1976) *Magnetic Resonance of Biomolecules*, p 225, Wiley, London.
Ladbrooke, B. D., & Chapman, D. (1969) *Chem. Phys. Lipids 3*, 304–357.
Lange, A., Marsh, D., Wassmer, K. H., Meier, P., & Kothe, G. (1985) *Biochemistry 24*, 4383–4392.

Lentz, B. R., Barenholz, Y., & Thompson, T. E. (1976) *Biochemistry 15*, 4529–4537.
Lentz, B. R., Moore, B. M., & Barrow, D. A. (1979) *Biophys. J. 25*, 489–494.
London, E., & Feigenson, G. W. (1981a) *Biochemistry 20*, 1932–1938.
London, E., & Feigenson, G. W. (1981b) *Biochim. Biophys. Acta 649*, 89–97.
Marsh, D. (1980) *Biochemistry 19*, 1632–1637.
Mason, J. T., Huang, C., & Biltonen, R. L. (1981) *Biochemistry 20*, 6086–6092.
McLaughlin, S., Mulrine, N., Gresalfi, G. V., & McLaughlin, A. (1981) *J. Gen. Physiol. 77*, 445–473.
Moore, W. J. (1962) in *Physical Chemistry*, 3rd ed., p 128, Prentice-Hall, Englewood Cliffs, NJ.
Morris, S. J., Smith, P. D., Gibson, C. G., Haynes, D. H., & Blumenthal, R. (1983) *Biophys. J. 41*, 28a.
Ohki, S. (1982) *Biochim. Biophys. Acta 689*, 1–11.
Ohki, S. (1984) *J. Membr. Biol. 77*, 265–275.
Ohnishi, S., & Tokutomi, S. (1981) *Biol. Magn. Reson. 3*, 121–153.
Papahadjopoulos, D., Vail, W. J., Newton, C., Nir, S., Jacobson, K., Poste, G., & Lazlo, R. (1977) *Biochim. Biophys. Acta 465*, 579–598.
Parasassi, T., Conti, F., Glaser, M., & Gratton, E. (1984a) *J. Biol. Chem. 259*, 14011–14017.
Parasassi, T., Conti, F., & Gratton, E. (1984b) *Biochemistry 23*, 5660–5664.
Parente, R. A., & Lentz, B. R. (1986) *Biochemistry 25*, 1021–1026.
Portis, A., Newton, C., Pangborn, W., & Papahadjopoulos, D. (1979) *Biochemistry 18*, 780–790.
Rand, R. P., Kachar, B., & Reese, T. S. (1985) *Biophys. J. 47*, 483–489.
Rintoul, D. A., Redd, M. B., & Wendelburg, B. (1986) *Biochemistry 25*, 1574–1579.
Savitzky, A., & Golay, M. J. E. (1964) *Anal. Chem. 36*, 1627–1639.
Shinitzky, M., & Barenholz, Y. (1978) *Biochim. Biophys. Acta 515*, 367–394.
Silvius, J. R., & Gagné, J. (1984a) *Biochemistry 23*, 3232–3240.
Silvius, J. R., & Gagné, J. (1984b) *Biochemistry 23*, 3241–3247.
Sklar, L. A., Hudson, B. S., & Simoni, R. D. (1977) *Biochemistry 16*, 819–828.
Sklar, L. A., Miljanick, G. P., & Dratz, E. A. (1979) *Biochemistry 18*, 1707–1716.
Teale, F. W. J. (1969) *Photochem. Photobiol. 10*, 363–374.
Tilcock, C. P. S., Bally, M. B., Faren, S. B., Cullis, P. R., & Gruner, S. M. (1984) *Biochemistry 23*, 2696–2703.
Tokutomi, S., Lew, R., & Ohnishi, S. (1981) *Biochim. Biophys. Acta 643*, 276–282.
Uster, P. S., & Deamer, D. W. (1981) *Arch. Biochem. Biophys. 209*, 385–395.
Welti, R., & Silbert, D. F. (1982) *Biochemistry 21*, 5685–5689.
Wilschut, J., Düzgünes, N., & Papahadjopoulos, D. (1981) *Biochemistry 20*, 3126–3133.
Yguerabide, J., & Foster, M. C. (1979) *J. Membr. Biol. 45*, 109–123.